

Collective modes of the extended Hubbard model with negative U and arbitrary electron density

T. Kostyrko and R. Micnas

Institute of Physics, A. Mickiewicz University, 60-780 Poznań, Poland

(Received 2 March 1992)

By use of a diagrammatic method we determine the density-density response functions in the random-phase approximation (RPA) and the collective-excitation spectrum for the extended Hubbard model with on-site attraction and arbitrary electron density, in the superconducting ground state. The energy of the collective modes, given by the poles of these response functions, is found to be a linear function of the wave vector (for small k and short-range intersite interaction) with the velocity interpolating smoothly between the weak- ($\propto 2zt$, $|U| \ll 2zt$) and strong-coupling ($\propto zt^2/|U|$, $|U| \gg 2zt$) limits. The latter agrees with the results obtained from an effective pseudospin Hamiltonian valid in the strong-coupling limit. The numerical analysis for a two-dimensional (2D) square lattice shows the occurrence of a roton-like minima near the zone boundary. In the weak-coupling regime we find that apart from a commensurate charge-density-wave (CDW) instability, an increase in the intersite Coulomb repulsion can give rise to a CDW incommensurate with the lattice period, away from half-filling. The resulting phase diagram for the 2D square lattice, including a singlet superconducting ground state, electronic-droplet formation, and CDW's, is determined. Finally, the effects of a long-range Coulomb interaction are analyzed briefly and it is shown that the energy of collective excitations evolves smoothly from the weak- to the strong-coupling limit for a 2D lattice.

I. INTRODUCTION

Presently known high-temperature superconductors are comprised of three groups of materials: the cuprates, doped bismuthates, and fullerenes. All of these materials generally exhibit low carrier density, a small value of the Fermi energy ($\propto 0.1-0.3$ eV), short coherence length ξ_0 , and they are strong type-II superconductors. The estimates based on the Fermi-liquid theory yield $\xi_0 k_F \propto 5-10$ (for 1:2:3 cuprates and fullerenes) which indicates that, in contrast to a weak-coupling BCS theory, the size of a pair is of the order of interparticle distance and that all carriers are practically involved in the pairing. Moreover, for high- T_c cuprates $T_c \propto n/m^*$ for low n (m^* being the effective mass and n the carrier density). These features of high- T_c materials strongly support the models with short-range, nonretarded attraction [see Ref. 1(a) for a review].

One of the simplest models of general interest is the extended Hubbard model with on-site attractive interaction.^{1(a)-3} It is a nontrivial model of fermions on the lattice which describes the transition from weak-coupling BCS-like superconductivity to the strong-coupling superconductor where the superconductivity results from the condensation of hard-core composite charged bosons and is similar to the superfluidity of ⁴He II.^{1(a),1(b)} Such a model has been considered as an effective model of superconductivity in CuO₂ planes,^{1(a),1(b),4(a)} of doped BaBiO₃,^{1,4(b)} and fullerenes.⁵

With the help of a canonical transformation, the extended negative- U Hubbard model can also be exactly mapped onto the positive- U half-filled band extended Hubbard model in an effective magnetic field.^{1(a),2} This attraction-repulsion transformation holds for the case of near-neighbor hopping on bipartite lattices and for any

electron density.

In this paper we determine the collective excitation spectrum of the extended Hubbard model over the superconducting ground state for arbitrary electron concentration. These collective modes are related to fluctuations of electron density and the phase of the superconducting order parameter. We will use the diagrammatic perturbation theory to calculate the density-density response function in the random-phase approximation (RPA). The collective excitations at $T=0$ K are analyzed in both the weak-coupling and strong-coupling limits and it is shown that they smoothly interpolate between the limits. Our numerical analysis is performed mainly for the two-dimensional (2D) square lattice and for nearest-neighbor Coulomb interaction. Finally, the effects of a long-range Coulomb interaction are discussed.

II. GENERAL RESULTS OF RANDOM-PHASE APPROXIMATION FOR RESPONSE FUNCTIONS

The extended one-band Hubbard model we study here is defined by the Hamiltonian:

$$\mathcal{H} - \mu N = \sum_{jm\sigma} t_{jm} c_{j\sigma}^\dagger c_{m\sigma} + U \sum_j n_{j\uparrow} n_{j\downarrow} + \sum_{j,m,\sigma,\sigma'} W_{jm} n_{j\sigma} n_{m\sigma'} - \mu \sum_{j,\sigma} n_{j\sigma}, \quad (1)$$

which takes the following form in \mathbf{k} space:

$$\mathcal{H} - \mu N = \sum_{\mathbf{k}\sigma} (\epsilon_{\mathbf{k}} - \mu) c_{\mathbf{k}\sigma}^\dagger c_{\mathbf{k}\sigma} + \frac{1}{2N_S} \sum_{\mathbf{k}\mathbf{p}\mathbf{q}\sigma\sigma'} (\delta_{-\sigma\sigma'} U + W_{\mathbf{q}}) \times c_{\mathbf{k}\sigma}^\dagger c_{\mathbf{k}+\mathbf{q}\sigma} c_{\mathbf{p}\sigma'}^\dagger c_{\mathbf{p}-\mathbf{q}\sigma'}. \quad (2)$$

In the above t_{jm} and W_{jm} denote the hopping integral and intersite density-density interaction, respectively, between sites j and m ; U is the on-site (attractive, $U < 0$) Hubbard interaction; μ is the chemical potential; and N and N_S are the number of electrons and lattice sites, respectively.

Energies of collective modes related to electron density oscillations are given by poles of the density-density response function:⁶

$$\tilde{\Pi}(\mathbf{q}, t) = -i\Theta(t) \sum_{\sigma\sigma'} \langle [\rho_{\mathbf{q}}^{\sigma}(t), \rho_{-\mathbf{q}}^{\sigma'}] \rangle, \quad (3)$$

where $\rho_{\mathbf{q}}^{\sigma}$ denotes the Fourier component of the electron density operator with spin σ . In the superconducting state, electron density oscillations are coupled to oscillations of phase and amplitude of a superconducting order parameter, which can be described by the operators $\Phi_{\mathbf{q}}$ and $A_{\mathbf{q}}$, respectively:

$$\Phi_{\mathbf{q}} = \rho_{\mathbf{q}}^{+} - \rho_{\mathbf{q}}^{-}, \quad (4)$$

$$A_{\mathbf{q}} = \rho_{\mathbf{q}}^{+} + \rho_{\mathbf{q}}^{-}, \quad (5)$$

where $\rho_{\mathbf{q}}^{+}$ ($\rho_{\mathbf{q}}^{-}$) denotes the Fourier transform of a pair creation (annihilation) operator:

$$\rho_{\mathbf{q}}^{+} = \frac{1}{N_S} \sum_{\mathbf{k}\sigma} c_{-\mathbf{k}+\mathbf{q}\uparrow}^{\dagger} c_{\mathbf{k}\uparrow}^{\dagger}, \quad \rho_{\mathbf{q}}^{-} = (\rho_{\mathbf{q}}^{+})^{\dagger}. \quad (6)$$

In order to account for this coupling we define a general response function in the form

$$\tilde{\Pi}^{\alpha\beta}(\mathbf{q}, t) = -i\Theta(t) \frac{1}{N_S^2} \sum_{\mathbf{k}\mathbf{p}} \langle [\Psi_{\mathbf{k}}^{\dagger}(t) \tilde{\tau}_{\alpha} \Psi_{\mathbf{k}+\mathbf{q}}(t), \Psi_{\mathbf{p}}^{\dagger} \tilde{\tau}_{\beta} \Psi_{\mathbf{p}-\mathbf{q}}] \rangle, \quad (7)$$

where $\Psi_{\mathbf{k}}^{\dagger}$ and $\Psi_{\mathbf{k}}$ denote two-component field operators in the Nambu representation, $\tilde{\tau}_{\alpha}$ are 2×2 matrices which form the following set:

$$\tilde{\Pi}^{\alpha\beta}(q) = \Pi^{\alpha\beta}(q)$$

$$+ \frac{[U + W_{\mathbf{q}} - U(U + 2W_{\mathbf{q}})\Pi^{\uparrow\uparrow}(q)][\Pi^{\downarrow\beta}(q)\Pi^{\alpha\uparrow}(q) + \Pi^{\uparrow\beta}(q)\Pi^{\alpha\downarrow}(q)] + [W_{\mathbf{q}} + U(U + 2W_{\mathbf{q}})\Pi^{\uparrow\uparrow}(q)][\Pi^{\uparrow\beta}(q)\Pi^{\alpha\uparrow}(q) + \Pi^{\downarrow\beta}(q)\Pi^{\alpha\downarrow}(q)]}{\{1 - U[\Pi^{\uparrow\uparrow}(q) - \Pi^{\downarrow\uparrow}(q)]\}\{1 - (U + 2W_{\mathbf{q}})[\Pi^{\uparrow\uparrow}(q) + \Pi^{\downarrow\uparrow}(q)]\}}, \quad (12)$$

which, in the particular case of the density-density response function, yields

$$\tilde{\Pi}(q) = \frac{\Pi(q)}{1 - (U/2 + W_{\mathbf{q}})\Pi(q)}, \quad (13)$$

$$\Pi(q) = \sum_{\sigma\sigma'} \Pi^{\sigma\sigma'}(q).$$

$$\tilde{\tau}_{\uparrow} = \begin{bmatrix} 1 & 0 \\ 0 & 0 \end{bmatrix}, \quad \tilde{\tau}_{\downarrow} = \begin{bmatrix} 0 & 0 \\ 0 & -1 \end{bmatrix}, \quad (8)$$

$$\tilde{\tau}_{+} = \begin{bmatrix} 0 & 1 \\ 0 & 0 \end{bmatrix}, \quad \tilde{\tau}_{-} = \begin{bmatrix} 0 & 0 \\ 1 & 0 \end{bmatrix}.$$

[We use matrices defined by Eq. (8) rather than more commonly used Pauli ones because, in our case, the interaction term (U) is the spin-dependent one.]

In this work we calculate the response functions by means of the diagrammatic method. For that purpose we define two-particle Matsubara Green functions corresponding to the retarded Green functions defined by Eq. (8):

$$\tilde{\Pi}^{\alpha\beta}(\mathbf{q}, \tau) = -\frac{1}{N_S^2} \sum_{\mathbf{k}\mathbf{p}} \langle T_{\tau} [\Psi_{\mathbf{k}}^{\dagger}(\tau) \tilde{\tau}_{\alpha} \Psi_{\mathbf{k}+\mathbf{q}}(\tau) \Psi_{\mathbf{p}}^{\dagger} \tilde{\tau}_{\beta} \Psi_{\mathbf{p}-\mathbf{q}}] \rangle. \quad (9)$$

as well as the Fourier transforms of Eq. (9), i.e., $\tilde{\Pi}^{\alpha\beta}(\mathbf{q}, i\omega)$. The original response functions can be obtained from the Matsubara functions by analytical continuation of $\tilde{\Pi}^{\alpha\beta}(\mathbf{q}, i\omega)$ to real frequencies. The perturbation expansion for the Matsubara function, $\tilde{\Pi}^{\alpha\beta}(\mathbf{q}, i\omega)$, with respect to $U + W_{\mathbf{q}}$ interactions leads to the following, formally exact equation:

$$\tilde{\Pi}^{\alpha\beta} = \Pi^{\alpha\beta} + \sum_{\sigma=\uparrow, \downarrow} \Pi^{\alpha\sigma}(U + W_{\mathbf{q}}) \tilde{\Pi}^{-\sigma\beta} + \sum_{\sigma=\uparrow, \downarrow} \Pi^{\alpha\sigma} W_{\mathbf{q}} \tilde{\Pi}^{\sigma\beta}, \quad (10)$$

where $\Pi^{\alpha\beta}$ denotes an (irreducible) polarization part:

$$\Pi^{\alpha\beta}(q) = \sum_{\mathbf{k}} \text{tr}[\mathcal{G}(k + q) \tilde{\tau}_{\alpha} \mathcal{G}(k) \Gamma^{\beta}(k, q)]. \quad (11)$$

In the above, $\mathcal{G}(k) = \mathcal{G}(\mathbf{k}, i\omega)$ denotes the one-particle Green function in the matrix Nambu representation, $\Gamma^{\beta}(k, q)$ is a full vertex part (defined here as the sum of all diagrams which are connected with the rest of a diagram with one interaction and two-particle lines and which cannot be cut into two by intersecting an interaction line). In Eq. (11) and in what follows $\sum_{\mathbf{k}} \equiv (1/N_S) \sum_{\mathbf{k}, i\omega}$.

Equation (10) can be formally solved to give

Subsequent analysis of Eqs. (12) and (13) requires knowledge of the vertex part, $\Gamma^{\beta}(k, q)$, and the one-particle Green functions which determine the polarization part [see Eq. (11)]. Here we calculate the polarization part in the RPA which leads to the following matrix integral equation for the vertex part:

$$\Gamma^{\beta}(q) = \tilde{\tau}_{\beta} - U \sum_{p\sigma} \tilde{\tau}_{-\sigma} \mathcal{G}(p) \Gamma^{\beta}(q) \mathcal{G}(p + q) \tilde{\tau}_{\sigma}. \quad (14)$$

In Eq. (14) we neglected the influence of the intersite term on $\Gamma^b(q)$. This is consistent with the fact that we neglect the \mathbf{k} dependence of the gap parameter, $\Delta_{\mathbf{k}}$, assuming that the effect of $U < 0$ is dominant in forming the superconducting state. The validity of this approximation for larger values of W_q (both repulsive and attractive) needs, however, more thorough examination which we left for our future work.

Following the RPA for the vertex part, we calculate a matrix self-energy $\Sigma(k)$ of the one-particle Green function $\mathcal{G}(k)$ in the (generalized) Hartree-Fock approximation (HFA):

$$\begin{aligned} \Sigma(k) = & \sum_{\sigma\sigma'} (\delta_{-\sigma\sigma'} U + W_0) \text{tr}[\vec{\tau}_\sigma \mathcal{G}(k)] \vec{\tau}_{\sigma'} \\ & + U \sum_{\sigma} \vec{\tau}_\sigma \mathcal{G}(k) \vec{\tau}_{-\sigma}. \end{aligned} \quad (15)$$

In order to obtain results consistent with Eq. (14), we had to omit in the Fock term of $\Sigma(k)$ both the normal and "anomalous" parts related to the intersite interaction W . A strategy based on the set of approximations, Eqs. (14) and (15), leads, in general, to results fulfilling conservation laws and is crucial for getting any reliable results concerning collective excitations (for a more complete discussion we refer the reader to the work of Baym and Kadanoff⁷ and Pines and Nozieres⁸).

The solution of Eq. (14) after inserting it into Eq. (11) leads to the following result for $\Pi(q)$:

$$\begin{aligned} \Pi(q) = & A(q) - D(q) \\ & + 2U \frac{[\Gamma(-q)B(q) + \Gamma(q)B(-q)]}{[1 - UC(q)][1 - UC(-q)] - U^2 D^2(q)}, \end{aligned} \quad (16)$$

where $\Gamma(q) = [1 - UC(q)]B(-q) + UD(q)B(q)$ and

$$A(q) = \sum_k \mathcal{G}_{11}(k+q) \mathcal{G}_{11}(k), \quad (17)$$

$$B(q) = \sum_k \mathcal{G}_{11}(k+q) \mathcal{G}_{21}(k), \quad (18)$$

$$C(q) = \sum_k \mathcal{G}_{11}(k+q) \mathcal{G}_{22}(k), \quad (19)$$

$$D(q) = \sum_k \mathcal{G}_{12}(k+q) \mathcal{G}_{12}(k). \quad (20)$$

In this paper we analyze the behavior of the collective modes in the ground state only—for this case Eqs. (17)–(20) together with Eq. (15) give [we put $i\omega \rightarrow \omega + i\delta$ in Eqs. (17)–(20) prior to taking $T \rightarrow 0$ K limit]

$$\begin{aligned} A(\mathbf{q}, \omega) = & \frac{1}{2N_S} \sum_{\mathbf{k}} (E_{\mathbf{k}-\mathbf{q}/2} E_{\mathbf{k}+\mathbf{q}/2} \\ & - \lambda_{\mathbf{k}-\mathbf{q}/2} \lambda_{\mathbf{k}+\mathbf{q}/2}) \beta_{\mathbf{k},\mathbf{q}}(\omega), \end{aligned} \quad (17a)$$

$$\begin{aligned} B(\mathbf{q}, \omega) = & \frac{-\Delta}{4N_S} \sum_{\mathbf{k}} (\lambda_{\mathbf{k}-\mathbf{q}/2} + \lambda_{\mathbf{k}+\mathbf{q}/2}) \beta_{\mathbf{k},\mathbf{q}}(\omega) \\ & - \frac{\omega\Delta}{4N_S} \sum_{\mathbf{k}} \beta_{\mathbf{k},\mathbf{q}}(\omega), \end{aligned} \quad (18a)$$

$$\begin{aligned} C(\mathbf{q}, \omega) = & \frac{1}{2N_S} \sum_{\mathbf{k}} (E_{\mathbf{k}-\mathbf{q}/2} E_{\mathbf{k}+\mathbf{q}/2} \\ & + \lambda_{\mathbf{k}-\mathbf{q}/2} \lambda_{\mathbf{k}+\mathbf{q}/2}) \beta_{\mathbf{k},\mathbf{q}}(\omega) \\ & - \frac{\omega}{2N_S} \sum_{\mathbf{k}} \left[\frac{\lambda_{\mathbf{k}-\mathbf{q}/2}}{E_{\mathbf{k}-\mathbf{q}/2}} + \frac{\lambda_{\mathbf{k}+\mathbf{q}/2}}{E_{\mathbf{k}+\mathbf{q}/2}} \right] \\ & \times \frac{1}{(E_{\mathbf{k}-\mathbf{q}/2} + E_{\mathbf{k}+\mathbf{q}/2})^2 - \omega^2}, \end{aligned} \quad (19a)$$

$$D(\mathbf{q}, \omega) = -\frac{\Delta^2}{4N_S} \sum_{\mathbf{k}} \beta_{\mathbf{k},\mathbf{q}}(\omega), \quad (20a)$$

where

$$\begin{aligned} \beta_{\mathbf{k},\mathbf{q}}(\omega) = & \left[\frac{1}{E_{\mathbf{k}-\mathbf{q}/2}} + \frac{1}{E_{\mathbf{k}+\mathbf{q}/2}} \right] \\ & \times \frac{-1}{(E_{\mathbf{k}-\mathbf{q}/2} + E_{\mathbf{k}+\mathbf{q}/2})^2 - \omega^2}, \end{aligned}$$

$E_{\mathbf{k}} = \sqrt{\lambda_{\mathbf{k}}^2 + \Delta^2}$ is a quasiparticle excitation energy, $\lambda_{\mathbf{k}} = \varepsilon_{\mathbf{k}} - \bar{\mu}$, and the gap parameter Δ and the chemical potential $\mu = \bar{\mu} + Un/2 + W_0 n$ ($n = N/N_S$) are determined from a set of HFA self-consistent equations:²

$$1 = -\frac{U}{2N_S} \sum_{\mathbf{k}} \frac{1}{E_{\mathbf{k}}}, \quad (21a)$$

$$1 - n = \frac{1}{N_S} \sum_{\mathbf{k}} \frac{\lambda_{\mathbf{k}}}{E_{\mathbf{k}}}. \quad (21b)$$

As follows from Eqs. (17a)–(20a), the polarization part is a real quantity provided that $\omega < \min_{\mathbf{k}} (E_{\mathbf{k}} + E_{\mathbf{k}+\mathbf{q}})$, where the last quantity determines the boundary of a quasiparticle continuum. Below this boundary and for small \mathbf{q}, ω , we may expand the lattice sums (17a)–(20a) in a Taylor series and insert the result into Eq. (16). We then obtain

$$\begin{aligned} \Pi(\mathbf{q}, \omega) = & \frac{1}{U} \mathbf{q}^2 \frac{\Delta^2 S_2(\hat{\mathbf{q}}) (\Delta^2 S_0^2 + U^2 S_1^2)}{\omega^2 (\Delta^2 S_0^2 + U^2 S_1^2) - \mathbf{q}^2 \Delta^2 U^2 S_2(\hat{\mathbf{q}}) S_0}, \\ & \mathbf{q} = \hat{\mathbf{q}}|\mathbf{q}|, \end{aligned} \quad (22)$$

where

$$S_0 = \frac{U^3}{N_S} \sum_{\mathbf{k}} \frac{1}{E_{\mathbf{k}}^3},$$

$$S_1 = \frac{U^2}{N_S} \sum_{\mathbf{k}} \frac{\lambda_{\mathbf{k}}}{E_{\mathbf{k}}^3},$$

$$S_2(\hat{\mathbf{q}}) = \frac{U}{N_S} \sum_{\mathbf{k}} \frac{(\hat{\mathbf{q}} \cdot \nabla \varepsilon_{\mathbf{k}})^2}{E_{\mathbf{k}}^3}.$$

Note that the lattice sums S_0 and S_1 can be computed using a density-of-state (DOS) function, $\mathcal{N}(\varepsilon)$. As concerns $S_2(\hat{\mathbf{q}})$, this simplification is possible for alternating hypercubic lattices (1d, 2d sq, 3d sc, bcc). In such a case we get⁹

$$S_2(\hat{\mathbf{q}}) = S_2 = \frac{2U}{Z\Delta^2} \int d\varepsilon \mathcal{N}(\varepsilon) \frac{\varepsilon(\varepsilon - \bar{\mu})}{\sqrt{(\varepsilon - \bar{\mu})^2 + \Delta^2}}, \quad (23)$$

where Z denotes the number of nearest neighbors.

III. COLLECTIVE MODES IN THE SYSTEM WITH SHORT-RANGE INTERSITE INTERACTION

A. Long-wavelength excitations

The energy of the collective modes is given by the pole of density-density response function [Eq. (13)] and, in the general case, it cannot be found analytically. In the case of long-wavelength excitations and a short-range interaction ($W_0 < \infty$), the collective modes make a gapless branch: $\Omega_q^2 = v^2 q^2$ with velocity v given by

$$v^2 = \Delta^2 S_2(\hat{q}) \frac{S_0 + (1/2)(1 + 2W_0/U)(\Delta^2 U^{-2} S_0^2 + S_1^2)}{\Delta^2 U^{-2} S_0^2 + S_1^2}. \quad (24)$$

The existence of this acoustic branch follows from the finite range of interaction in the system and the continuous degeneracy of the superconducting ground state and exemplifies a nonrelativistic Goldstone theorem.¹⁰ If we assume a quadratic dispersion of the one-electron spectrum, Eq. (24) leads in the weak- U limit to a result closely resembling a weak-coupling formula of Anderson for the BCS superconductor:¹¹

$$v^2 = \frac{1}{d} v_F^2 [1 + (U + 2W_0)\mathcal{N}(\epsilon_F)] \quad (25)$$

(d is the lattice dimension). In the lattice model Eq. (25) is valid in a low-density limit only, where the quadratic approximation for ϵ_k can be reasonably applied. For larger values of electron density we can use a constant DOS function to estimate integrals S_α . We obtain that $v \rightarrow 4t\sqrt{n(2-n)}/Z$, for $U, W_0 \rightarrow 0$. In general, the velocity of the collective modes, considered as a function of U , goes smoothly from the value of the order of the bandwidth, for $|2Zt/U| > 1$, to the result of the strong-coupling theory (Bogoliubov mode) [Ref. 1(a)], which is based on an effective Heisenberg Hamiltonian exact (for $|t/U| \ll 1$) up to terms of order $t^2/|U|$:

$$v^2 = \frac{8}{Z} \frac{t^4}{U^2} \left[1 + \frac{W|U|}{2t^2} \right] n(2-n) \quad (26)$$

[W is the nearest-neighbor (NN) interaction]. This conclusion has been reached analytically in our previous work⁹ (see also Ref. 12) to hold for all alternating lattices. In Fig. 1(a), we present the numerical results for v vs n for the two-dimensional (2D) nearest-neighbor square (sq) lattice. The nonmonotonous increase of $v(n)$ in the weak-coupling range is the effect of the singularity in the 2D density of states for the NN lattice. For larger values of U , the particular shape of a DOS becomes less important and the $v(n)$ plot steadily approaches the result of the perturbation theory [Eq. (26)]. The fact that the RPA interpolates smoothly between the two limits is related to an analogous behavior of the Hartree-Fock (BCS) ground state^{2,9,13} above which the collective modes are created in the present theory. Thus, we conclude that there is no sharp distinction between the weak- and strong-coupling superconductivity in the negative- U Hubbard model at $T=0$ K.

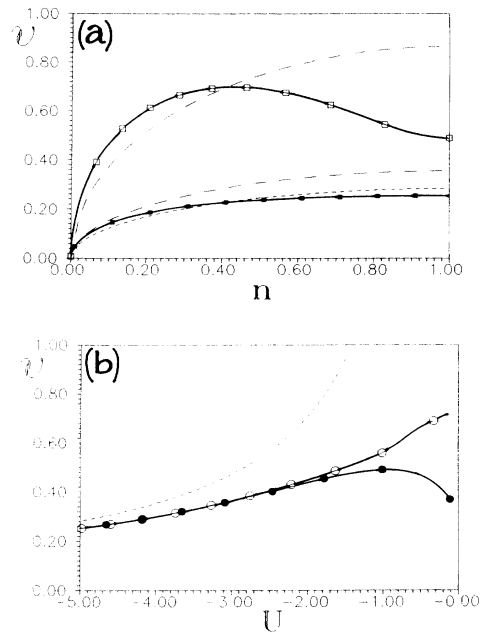


FIG. 1. (a) The velocity of the collective modes (v) as a function of the electron density (n) for two values of attraction U and $W=0$ ($U=-1$, open squares; $U=-5$, solid squares). For a comparison the result of the strong-coupling theory [Refs. 1(a) and 2] for $U=-5$ is shown as a short-dashed line. Long-dashed lines approaching the solid curves for $n \rightarrow 0$ are estimations of v for the square DOS for the two values of U . Here and in the next figures we use $|2t|$ as our energy unit. (b) The velocity v as a function of U ($W=0$) for $n=1$ (solid circles) and $n=0.8$ (open circles). The short-dashed line shows the result of the strong-coupling theory for $n=1$.

In some cases it may happen that the position of the Fermi energy coincides with a singularity in the DOS. Neither Eq. (24) nor the corresponding formula obtained for a constant DOS can be used then. In the case of a 2D sq lattice and $n=1$, ϵ_F lays exactly in the middle of the band and coincides with a position of logarithmic singularity of $\mathcal{N}(\epsilon)$. The integrals S_α can be calculated using a logarithmic approximation to $\mathcal{N}(\epsilon)$:

$$\mathcal{N}(\epsilon) = \mathcal{N} \ln |16t/\epsilon| \quad (27)$$

(\mathcal{N} is a normalization constant). Equation (21) then has the following approximate solution for the gap parameter Δ , which is valid in the weak- U limit:

$$\Delta = 32t \exp[-\sqrt{2/\mathcal{N}|U| + \ln^2(4)}], \quad (28)$$

whereas Eq. (24) gives

$$v^2 = \frac{4[4 \ln(2) + 1]}{2 \ln(32t/\Delta)} t^2. \quad (29)$$

Taking into account Eq. (28), $v \propto |U|^{1/4}$, i.e., $v \rightarrow 0$ for $U \rightarrow 0$. The last conclusion also holds for the bcc lattice and may also be true in some other cases for $n \neq 1$ provided that ϵ_F coincides with a position of a strong van Hove singularity in $\mathcal{N}(\epsilon)$. It is of interest to observe that this result is in sharp contrast to the case of the lattices with

finite $\mathcal{N}(\varepsilon_F)$ for which ν tends to a finite limit for $U \rightarrow 0$ (being the first sound for fermions⁶).

For $n=1$, the negative- U model can be exactly mapped into the positive- U one while the superconducting s -wave state is transformed into an antiferromagnetic (AF) state ordered in the XY plane.^{1(a),2} The energy of the collective excitations related to oscillations of the phase of the superconducting order parameter and electron density in the $U < 0$ Hubbard model will then correspond to the energy of spin-wave excitations in the AF state. The velocity of the antiferromagnetic spin waves in the positive- U Hubbard model was calculated by many authors.¹⁴ In particular, our Eq. (24) would be exactly the same as a corresponding formula for the velocity in the work of Yamada and Shimizu¹⁴ [cf. Eqs. (40)–(44) of their work] if we put $\bar{\mu} = S_1 = W_0 = 0$ here. In the same context, Johansson and Berggren¹⁴ calculated the velocity for a 1D chain and noted that the transition between the strong- U and weak- U limits was continuous. However, the peculiar behavior of ν in connection with the van Hove singularity seems to pass unnoticed in these works.

In Fig. 1(b), we present the numerical results for ν vs U for the sq lattice for several values of n showing again the continuous transition from the weak- to strong- U limit and the effect of the singular DOS for $n = 1$.

B. Intermediate- and short-wavelength excitations

For the sake of clarity of the foregoing discussion, we shall consider first collective modes in the simple Hubbard model. The overall \mathbf{q} dependence of $\Omega_{\mathbf{q}}$ relies upon electron band filling. The most prominent feature of the $\Omega_{\mathbf{q}}$ plot for $n = 1$ is the complete softening of the collective excitation branch for $\mathbf{q} \rightarrow \mathbf{M} = (\pi, \pi)$ for arbitrary U . This reflects the degeneracy of the superconducting s -wave state and a commensurate charge-density-wave (CDW) state which is the exact property of the simple Hubbard Hamiltonian for the half-filled band. As n starts to depart from unity, the absolute minimum at $\mathbf{q} = \mathbf{M}$ turns to a local one; then, at some critical electron density ($n = 1 - \sqrt{3}/3$ in the strong- $|U|$ limit), it changes to a local maximum. The exact energy of the collective mode for this particular wave vector can be easily calculated directly—on the assumption that the superconducting state is a stable one—using the fact that the pair creation operator, $\rho_{\mathbf{q}}^\dagger$, is an exact eigenoperator of the Hubbard Hamiltonian for $\mathbf{q} = \mathbf{M}$:¹⁵

$$\mathcal{H}\rho_{\mathbf{M}}^\dagger = (U - 2\mu)\rho_{\mathbf{M}}^\dagger,$$

giving $\Omega_{\mathbf{q}} = U - 2\mu$. This last equality is also strictly fulfilled by our RPA results provided that we substitute the exact chemical potential, μ , by the approximate HFA one. This formal agreement between our results and the exact ones can easily be shown using the complete equivalence of the diagrammatic formulation of the RPA with the one based on the equation of motion for the real-time response functions.⁹

The typical behavior of $\Omega_{\mathbf{q}}$ along the lines of the high symmetry of the Brillouin zone of the 2D tight-binding square lattice is shown in Fig. 2 for different values of

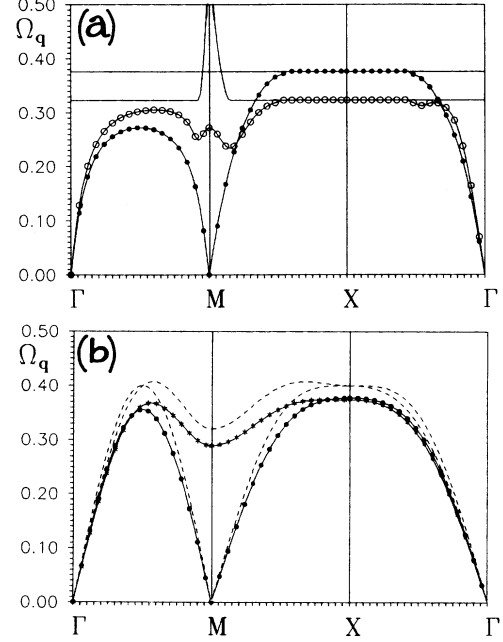


FIG. 2. (a) The energy of the collective modes ($\Omega_{\mathbf{q}}$) as a function of the wave vector (\mathbf{q}) along the directions of high symmetry for the 2D square lattice for $U = -1$, $W = 0$, and two values of the electron density ($n = 1$, solid circles; $n = 0.8$, open circles). The boundary of the one-particle excitation continuum is shown as a simple solid line for each n . (b) The energy of the collective modes ($\Omega_{\mathbf{q}}$) as a function of the wave vector (\mathbf{q}) for $U = -5$, $W = 0$, and two values of the electron density ($n = 1$, solid circles; $n = 0.6$; stars). The short-dashed lines show the results of the strong-coupling theory for each n .

electron density n for values of U corresponding to the weak-coupling [$U = -2|t|$, Fig. 2(a)] and the strong-coupling [$U = -10|t|$, Fig. 2(b)] ranges. A linear \mathbf{q} dependence of $\Omega_{\mathbf{q}}$ is clearly seen in the small- \mathbf{q} range. In the case of the strong interaction, the dispersion curves approach values obtained with the help of an effective pseudospin Hamiltonian,² which are given by

$$\Omega_{\mathbf{q}} = \frac{2Zt^2}{|U|} \sqrt{(1 - \gamma_{\mathbf{q}})[1 - \gamma_{\mathbf{q}}(2n^2 - 4n + 1)]}, \quad (30)$$

$$\gamma_{\mathbf{q}} = \frac{1}{Z} \sum_{\delta} e^{i\mathbf{q} \cdot \delta}$$

(δ is an elementary unit lattice vector). A maximum value of the collective excitation energy is then of order $\nu \propto t^2/|U|$, which is far below the boundary of the quasiparticle excitations continuum, $\min_{\mathbf{k}}(E_{\mathbf{k}} + E_{\mathbf{k}+\mathbf{q}}) > 2\Delta \approx |U|$. The picture changes in the weak-coupling limit. The boundary of quasiparticle continuum decreases, whereas the maximum value of $\Omega_{\mathbf{q}}$ increases with the decrease of $|U|$, and finally the dispersion curve of $\Omega_{\mathbf{q}}$ sticks to the continuum. As our numerical results show, the $\Omega_{\mathbf{q}}$ curve does not cross the continuum boundary for any value of U . Analytically, this is related to the fact that all lattice sums, Eqs. (17a)–(20a), diverge for $\omega \rightarrow \min_{\mathbf{k}}(E_{\mathbf{k}} + E_{\mathbf{k}+\mathbf{q}})$ making the denominator of the density-density response function [Eq. (13)] change sign

in an interval: $0 < \omega < \min_{\mathbf{k}}(E_{\mathbf{k}} + E_{\mathbf{k}+\mathbf{q}})$. In effect, we find in the energy gap, the collective mode with an infinite lifetime for arbitrary \mathbf{q} , n , U . The importance of this undamped mode may be limited, however, by a small value of its spectral weight.

One more striking difference between the weak- and strong-coupling behavior of the excitation energy is the existence of an apparent depression on the weak-coupling curves seen for several wave vectors inside the first Brillouin zone. These depressions—resembling rotonlike minima—evolve from the original minimum at $\mathbf{q}=\mathbf{M}$ as n moves from unity. They can be interpreted as incomplete soft modes and indicate a tendency towards the formation of an incommensurate CDW. In the simple Hubbard model this tendency is not strong enough to stabilize a long-range incommensurate CDW state, but it can be greatly enhanced by the repulsive intersite interactions, as will be discussed in the next section.

C. Instability with respect to CDW

We start our analysis of the influence of the intersite interaction on $\Omega_{\mathbf{q}}$ with an observation that—to a first approximation— $W_{\mathbf{q}}$ can be represented as a \mathbf{q} -dependent shift of the intrasite term [cf., Eq. (13)]. In general, there are some regions of \mathbf{q} values in the Brillouin zone (BZ) for which $W_{\mathbf{q}}$ is negative and effectively enhances U , as well as regions of $W_{\mathbf{q}} < 0$, where U is reduced by $W_{\mathbf{q}}$. To be more specific, we consider first the NN interaction on the sq lattice:

$$W_{\mathbf{q}} = W_0/2[\cos(k_x) + \cos(k_y)],$$

with positive W_0 . In this case, $W_{\mathbf{q}}$ is positive inside the square domain of the BZ defined by four inequalities: $k_y > \mp k_x - \pi$, $k_y < \pm k_x + \pi$, which has the Γ point in its center. In result $W_{\mathbf{q}}$ enhances $\Omega_{\mathbf{q}}$ within this domain and reduces outside it—therefore, the velocity of the collective modes will be increased by intersite repulsion [cf., Eqs. (26) and (25)] but the minima of $\Omega_{\mathbf{q}}$ found near the \mathbf{M} point will still be more depressed (see Fig. 3). This tendency is even more pronounced for larger values of

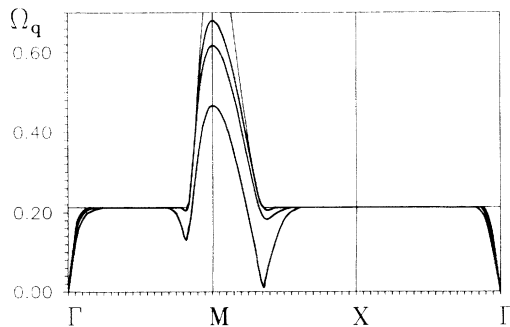


FIG. 3. The energy for the collective modes ($\Omega_{\mathbf{q}}$) for $U = -1$, $n = 0.6$, and three values of W_0 (this solid lines: $W_0 = 0$, $W_0 = W_0^c/2$, and $W_0 \approx W_0^c$, where W_0^c denotes a value for which $\Omega_{\mathbf{q}}$ softens completely for this U and n). The figure shows the deepening of the local minimum in the $\Omega_{\mathbf{q}}$ curves in the interval \mathbf{MX} with the increase of W_0 . The thin solid line shows the boundary of the one-particle continuum.

$W_{\mathbf{q}}$ where representing an intersite term as a mere shift of U is not well justified. Eventually, for some critical value of $W_{\mathbf{q}}$ depending upon the $|U/t|$ ratio and the electron density n , the collective mode energy can soften completely for some critical wave vector \mathbf{q}^c . This effect is most clearly seen in the strong- U limit where $\Omega_{\mathbf{M}}$ goes to zero first for

$$W_0^c = \frac{2Zt^2}{|U|} \frac{(1-n)^2}{1-(1-n)^2}. \quad (31)$$

Softening at $\mathbf{q}^c = \mathbf{M}$ means that the simple s -wave state becomes unstable with respect to the formation of the commensurate CDW. In the resulting ground state, the electron charge density alternates along lattice directions, and the superconducting order parameter is still nonzero². The situation is, however, different in the small- U limit where the critical value of the wave vector depends almost linearly on electron density. From Eq. (13), W_0^c can be determined as an absolute minimum in the BZ of a function:

$$W_{\mathbf{q}}^c = \frac{1}{\gamma_{\mathbf{q}}} \left[\frac{1}{\Pi(\mathbf{q}, 0)} - \frac{U}{2} \right]. \quad (32)$$

We may thus expect the formation of a new superconducting state accompanied by an incommensurate CDW for $W_0 > W_0^c$. The appearance of the incommensurate CDW is a feature of the phase diagram of the extended Hubbard model which has not been previously discussed. In Fig. 4 we marked the phase boundaries of commensurate and incommensurate CDW's obtained from RPA-HFA theory for the sq lattice. We note that a similar effect of softening of the collective excitation energy at

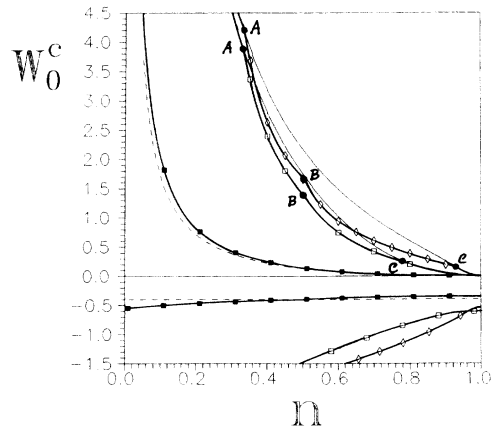


FIG. 4. Boundaries of stability of the s -wave state in the W_0-n parameter plane for three values of U ($U = -5$, solid squares and also a short-dashed line showing the limit of the strong-coupling theory; $U = -1$, open squares; $U = -0.5$, diamonds). The s -wave state is stable between the line of droplet instability (for $W_0 < 0$) and the line of CDW instability (for $W_0 > 0$). Between points B and C of the latter curves, softening of $\Omega_{\mathbf{q}}$ takes place along the \mathbf{MX} direction of the Brillouin zone, between A and B it takes place along the \mathbf{GM} direction. In the rest of these curves $\Omega_{\mathbf{q}}$ softens exactly at the corner of the BZ first. Thin solid lines connecting points A and C show where $\Omega_{\mathbf{M}}$ goes to zero.

$q^c \neq \mathbf{M}$ was also analyzed in the simple Hubbard model for the repulsive U (and $n \neq 1$) by Shulz.¹⁶ He determined the stability of a simple antiferromagnetic state with respect to an incommensurate spin-density wave (SDW) and found a SDW with a modulation along the \mathbf{MX} direction of the BZ to always be the most stable one [$\mathbf{X}=(\pi,0)$]. However, for the extended Hubbard model with $U < 0$, we find that the incommensurate CDW with a periodic modulation of electron density along the $\Gamma\mathbf{M}$ direction can be more stable for smaller electron densities than an analogous CDW with \mathbf{q} along the \mathbf{MX} direction.

Another type of instability which occurs in the system for the negative W_0 is a phase separation or electron-“droplet” formation. With increasing $|W_0|$, the velocity v decreases then [cf. Eqs. (25) and (26)], and upon reaching a critical value of $W_0 = W_0^d$ it becomes imaginary, indicating the instability of the superconducting state. Similarly as in the strong-coupling theory, the superconductivity disappears for $|W_0| > |W_0^d|$ and electrons in the system form a single cluster then (a droplet state).

Our RPA analysis of the energy of Ω_q allows us to determine boundaries separating the simple s -wave superconducting phase and the other discussed phases in the whole range of n and $|t/U|$. The result of our computations for the NN sq lattice is shown in Fig. 4. As one can see, the present results are very close to those obtained within the strong-coupling theory already for $|U/2Zt|=1.25$. In the weak-coupling limit the phase diagram is qualitatively improved by including incommensurate CDW's as compared to the simple Hartree-Fock theory of Robaszkiewicz, Micnas, and Chao.²

IV. COMMENTS ON THE EFFECTS OF LONG-RANGE INTERACTIONS

At least since the work of Anderson¹¹ it is well known that, in the long-wavelength limit, the long-range Coulomb interactions push the collective modes up to a region of ordinary plasma oscillations. This result is valid for isotropic 3D systems and one can easily see from our general expressions for the response function, Eqs. (13) and (22), how it comes about. The q^{-2} divergence of the Fourier transform of the intersite Coulomb term, $W_q = 4\pi e^2/q^2$, is cancelled by the q^2 term in the numerator of the polarization part [Eq. (22)] leading to a constant term in the denominator of the response function [Eq. (13)] in the limit $|\mathbf{q}| \rightarrow 0$. As a consequence, the response function can have a divergence for a finite value of ω only. In order to determine precisely the value of this divergence—and hence the plasmon energy—one has to expand the polarization part [Eq. (16)] in a Taylor series around $\mathbf{q}=0$ for finite ω . The quantitative analysis of this problem needs a detailed specification of the form of the long-range interaction and the particular lattice structure and will be presented in a separate work. Here we want to point out the qualitative dependence of the excitation energy on the dimensionality of the lattice structure. In a strictly 2D system, the divergence of the Fourier transform of the long-range term weakens and W_q changes to $W_q = 2\pi e^2/|\mathbf{q}|$, which no longer cancels the q^2 term in the numerator of Eq. (22). As a result, one

has an “acoustic” plasmon branch with a square-root dispersion:

$$\Omega_q = \sqrt{|\mathbf{q}| 2\pi e^2 \Delta^2 S_2 / U} . \quad (33)$$

The quadratic one-electron dispersion calculation of S_2 is straightforward and gives, in the $\Delta \rightarrow 0$ limit

$$S_2 = \frac{Un}{\Delta^2 m^*} \quad (34)$$

(m^* is an effective electron mass), which, inserted to Eq. (33), reproduces a familiar result for the 2D interacting electron gas:

$$\Omega_q = \sqrt{2\pi n e^2 |\mathbf{q}| / m^*} \quad (35)$$

(Crandall¹⁷). In the opposite limit of the strong on-site attraction, $\Delta^2 S_2 / U$ can be approximated by $4t^2 n(2-n)/|U|$,⁹ and we again rederive the result of the strong-coupling theory:^{1(a)}

$$\Omega_q = \sqrt{2\pi e^2 |\mathbf{q}| 4t^2 n(2-n)/|U|} . \quad (36)$$

This extends our conclusion about a continuous transition between weak- and strong- U limit to the case of the long-range intersite interactions. Finally, in the particular case of the NN sq lattice, we can use Eq. (23) to derive a simple explicit formula for Ω_q which interpolates between the two limits:

$$\Omega_q = \left[|\mathbf{q}| \pi e^2 \int d\varepsilon \mathcal{N}(\varepsilon) \frac{\varepsilon(\varepsilon - \mu)}{(\varepsilon - \mu)^2 + \Delta^2} \right]^{1/2} . \quad (37)$$

Note that, in this case Ω_q —unlike the short-range interaction case—remains finite for $n=1$ in the $U \rightarrow 0$ limit despite the logarithmic singularity in the DOS.

Let us now consider a system of 2D layers with the isotropic long-range Coulomb interaction within the layers and between them—which is roughly the case of the copper-oxide superconductors. Now the interaction can be approximately represented by $W_q = 4\pi e^2 / (q_{\parallel}^2 + q_{\perp}^2)$, where q_{\parallel} and q_{\perp} denote components of the wave vector parallel and perpendicular to the layers, respectively. For a finite constant value of q_{\perp} , W_q can be treated as a q_{\parallel} -dependent short-range interaction within the layers. As was noted by Fertig and Das Sarma,¹⁸ a branch of collective modes with arbitrary small energy for $q_{\parallel} \rightarrow 0$ and constant q_{\perp} should exist in the gap in such a case. This conclusion may change if we allow electrons to hop between the layers. We expect that there is a critical value of the interplane to intraplane hopping ratio for which density oscillations with finite q_{\perp} and $q_{\parallel} \rightarrow 0$ would be pushed out from the gap. This problem can be studied systematically with the help of our general RPA expressions for the density-density response function, Eqs. (13) and (22).

V. DISCUSSION

In conclusion, we recall the main points of this paper and briefly reexamine the validity and significance of our findings.

(1) Using the method of perturbation expansion, we calculated the density-density response functions for the

extended Hubbard model with negative U in the random phase approximation. The result we obtained [Eqs. (13) and (16)–(20)] is valid for an arbitrary lattice structure and electron density both in the normal and in the superconducting s -wave state. We also obtained simple explicit formulas for the response functions for the superconducting ground state as well as their expansion for small values of ω and q . Our results may find a general application in the analysis of the electromagnetic properties of superconductors with local pairing.

A shortcoming of our analysis is that we neglected the anisotropy of the superconducting order parameter in the evaluation of the irreducible polarization [cf., Eq. (14)]. This simplification is not important in the limiting case of the strong coupling or for $W \ll |U|$, but may be more serious in the intermediate region. Besides, there are many experiments on the copper-oxide superconductors (tunneling,¹⁹ NMR relaxation²⁰), suggesting that considering an anisotropy of the gap parameter is necessary to explain the data. We hope to be able to clarify a possible role of the gap anisotropy in our future work.

(2) Knowing the poles of the response functions, we calculated the energy of collective modes related to the oscillations of the electron density and to the phase and amplitude of the order parameter in the superconducting ground state. We found that the energy evolves from the weak- to strong-coupling limit in a continuous way. This result holds both for the short- and long-range intersite Coulomb interactions. The validity of our conclusion is so far restricted to the ground state only and an adequate theory for the finite-temperature region is yet to be

found. We also note that the possible role of nonlinear solutions, like localized pairing bag excitations in a 2D lattice,^{4(a)} is beyond the scope of the present RPA approach.

(3) We performed a numerical analysis of the q -vector dependence of the collective mode energy and determined the condition of the stability of the spectrum and, hence, the s -wave state in the wide range of values of model parameters and electron densities. For the strong enough intersite NN interaction W and the 2D sq lattice, the “pure” s -wave state was found to be unstable with respect to the formation of either the commensurate or incommensurate charge-density-wave state (for the repulsive W) or to electron-droplet formation (in the opposite case). At present we cannot definitely tell whether the incommensurate phases would persist in the isotropic (e.g., sc) lattice and an answer to this will require much more numerical effort. As for the possible influence of the long-range Coulomb interaction on the stability of these phases, the result will depend on the short-wavelength dependence of W_q —that is, on details of a considered model of this term.

ACKNOWLEDGMENTS

We would like to express our gratitude to Professor S. Robaszkiewicz for very valuable discussions. We gratefully acknowledge the financial support of the Committee of Scientific Research (K.B.N.) within the Project Nos. 200 11 91 01 and 200 68 91 01.

- ^{1(a)}R. Micnas, J. Ranninger, and S. Robaszkiewicz, *Rev. Mod. Phys.* **62**, 113 (1990); (b) N. F. Mott, *Adv. Phys.* **39**, 55 (1991); L. J. de Jongh, *Physica C* **152**, 171 (1988); **161**, 631 (1989).
- ²R. Robaszkiewicz, R. Micnas, and K. A. Chao, *Phys. Rev. B* **23**, 1447 (1981); **24**, 1579 (1981); **24**, 4018 (1981); **26**, 3915 (1982).
- ³R. T. Scalettar *et al.*, *Phys. Rev. Lett.* **62**, 1407 (1989).
- ^{4(a)}A. R. Bishop, P. S. Lomdahl, J. R. Schrieffer, and S. A. Trugman, *Phys. Rev. Lett.* **61**, 2709 (1988); (b) C. M. Varma, *ibid.* **61**, 2713 (1988).
- ⁵S. Chakravarty and S. Kivelson, *Europhys. Lett.* **16**, 751 (1991); F. C. Zhang, M. Ogata, and T. M. Rice, *Phys. Rev. Lett.* **67**, 3452 (1991); J. A. Wilson, *Physica C* **182**, 1 (1991).
- ⁶J. R. Schrieffer, *Theory of Superconductivity* (Benjamin, New York, 1964); A. L. Fetter and J. D. Walecka, *Quantum Theory of Many-Particle Systems* (McGraw-Hill, New York, 1971).
- ⁷G. Baym and L. P. Kadanoff, *Phys. Rev.* **124**, 287 (1961).
- ⁸D. Pines and P. Nozières, *The Theory of Quantum Liquids* (Benjamin, New York, 1966).
- ⁹T. Kostyrko, *Phys. Status Solidi (B)* **135**, K79 (1986); **143**, 149

- (1987).
- ¹⁰R. V. Lange, *Phys. Rev.* **146**, 301 (1966); J. B. Johansson, *J. Phys. C* **3**, 50 (1970).
- ¹¹P. W. Anderson, *Phys. Rev.* **112**, 1900 (1958).
- ¹²K. Nasu, *Physica B* **143**, 229 (1986).
- ¹³P. Nozières and S. Schmitt-Rink, *J. Low Temp. Phys.* **59**, 195 (1985); M. Randeria, J.-M. Duan, and L.-Y. Shieh, *Phys. Rev. Lett.* **62**, 981 (1989); *Phys. Rev. B* **41**, 327 (1990).
- ¹⁴A. K. Rajagopal, *Phys. Rev.* **137**, A1429 (1965); B. Johansson and K. F. Berggren, *ibid.* **181**, 855 (1969); J. B. Sokoloff, *ibid.* **185**, 770 (1969); H. Yamada and M. Shimizu, *J. Phys. Soc. Jpn.* **42**, 749 (1977).
- ¹⁵S. Zhang, *Phys. Rev. Lett.* **65**, 120 (1990).
- ¹⁶H. J. Schulz, *Phys. Rev. Lett.* **64**, 1445 (1990).
- ¹⁷R. S. Crandall, *Phys. Rev. A* **8**, 2136 (1973).
- ¹⁸H. A. Fertig and S. Das Sarma, *Phys. Rev. Lett.* **65**, 1482 (1990).
- ¹⁹M. Boekholt *et al.*, *Physica C* **175**, 127 (1991).
- ²⁰Y. Kitaoka *et al.*, *Physica C* **153-155**, 83 (1988); P. C. Hammel *et al.*, *Phys. Rev. Lett.* **63**, 1992 (1989).